

Contents lists available at ScienceDirect

Sensing and Bio-Sensing Research

journal homepage: www.elsevier.com/locate/sbsr

Proposal of a gas sensor with high sensitivity, birefringence and nonlinearity for air pollution monitoring



Sayed Asaduzzaman, Kawsar Ahmed *

Department of Information and Communication Technology, Mawlana Bhashani Science and Technology University, Santosh, Tangail 1902, Bangladesh

ARTICLE INFO

Article history:

Received 1 May 2016

Received in revised form 4 June 2016

Accepted 29 June 2016

Keywords:

Gas sensor

Air pollution sensing

Birefringence

Nonlinear coefficient

Sensitivity

Photonic crystal fiber

ABSTRACT

Flammable or poisonous gasses in the air are capable of destroying a geographical area of causing a fire, fulmination, and venomous exposure. This paper presents a micro-cored photonic crystal fiber based gas sensor for detecting colorless or toxic gasses and monitoring air pollution by measuring gas condensate components in production facilities. The numerical investigation of the proposed PCF takes place using the finite element method (FEM). The geometrical parameters of proposed PCF are varied to optimize and observe the dependence of guiding properties on them. According to simulated results, the high relative sensitivity of 53.07% is obtained at 1.33 μm wavelength for optimum parameters. In addition, high birefringence of the order 6.9×10^{-3} ; lower confinement loss of 3.21×10^{-6} dB/m is also gained at the same wavelength. Moreover, nonlinear coefficient, effective area, splice loss, V parameters and beat length are reported briefly.

© 2016 The Authors. Published by Elsevier B.V. This is an open access article under the CC BY-NC-ND license (<http://creativecommons.org/licenses/by-nc-nd/4.0/>).

1. Introduction

Recently, due to the advancement of technology and for an extra degree of freedom photonic crystal fiber has drawn the attention of the researchers. Photonic crystal fiber (PCF) or holey fibers (HFs) or microstructure optical fiber contains a microscopic array of air channels that run through the entire fiber and formulates a lower index cladding on a silica background [1]. According to the guiding mechanism, PCF can be divided into two categories. One is photonic bandgap fiber (PBG) [2, 3] where the light is guided by photonic bandgap principle and another is index guiding (IG) PCF [4,5] where light can be guided through low index core by photonic crystal reflection cladding. Although the first fabricated PCF was hexagonal [6] but for encouraging technology, a lot of design flexibility is now possible. So to achieve better-guiding properties octagonal [7], decagonal [8], honeycomb cladding [9], circular [10] and hybrid [11] shaped PCF is designed nowadays. So far, high sensitivity [12], high birefringence [13], ultra-flattened dispersion [14], high nonlinear effect [15] can be accomplished by designing PCF because the advanced manufacturing technology allows PCF to tune by varying the air hole diameters and pitch. PCFs can be used for optical communication [16], nonlinear optics [17], high power technology [18], spectroscopy [19], supercontinuum generation [20], sensing application like - gas sensing [21] and chemical sensing [7] for its unique properties.

Microstructure core and cladding were first introduced by Cordeiro et al. [22] which shows that this type of PCF helps to increase energy into the holes which contain gas. An index-guiding PCF (IG-PCF) based gas sensor was proposed [23] which show a relative sensitivity of 13.23% and confinement loss of 3.77×10^{-6} . In 2015, M. Morshed et al. proposed a modified photonic crystal fiber [24] of [25] for gas sensing which shows better sensitivity and lowers confinement loss. The proposed PCF contains microstructure core instead of hollow core (of prior PCF) which improves the relative sensitivity of 42.27% with a lower confinement loss of 4.78×10^{-6} . Both the structures [23,25] demonstrate that by increasing the diameters of air holes placed in inner ring results in high relative sensitivity, whereas by increasing the air holes placed in outer ring results degraded confinement loss. A novel design of PCF was proposed in [26] where both core and cladding contains elliptical holes formed horizontally and vertically which shows high relative sensitivity, high birefringence and lower confinement loss simultaneously. The proposed PCF was used as a liquid analyte (water, ethanol and benzene) sensor.

A hybrid photonic crystal fiber was proposed in [27] which show birefringence of 3.79×10^{-2} and high nonlinearity of $40.1 \text{ W}^{-1} \text{ km}^{-1}$ at the wavelength of 1.55 μm . In [13], hybrid cladding PCF was proposed where the holes of the cladding wherein different shapes and used for dispersion, a nonlinear effect, birefringence and effective area. High birefringent PCFs can easily be realized for design flexibility and high index contrast. There are lots of significant applications of high birefringent PCFs such as - fiber sensors, fiber filters, fiber communication etc. By depicting an asymmetric solid fiber core which is surrounded by air holes having double/triple defect core of PCF can be shaped for

* Corresponding author.

E-mail addresses: samonna25@gmail.com (S. Asaduzzaman),kawsar_it08050@yahoo.com, kawsar.ict@mbstu.ac.bd, kawsarit08050@gmail.com (K. Ahmed).

achieving high birefringence [28]. On the other hand, several papers show that ultrahigh birefringence can be gained by applying elliptical holes [28]. It is not easy to fabricate PCFs with elliptical holes accurately [29]. In addition, birefringence study in PCFs is growing interest day by day. The design of PCFs with high nonlinear coefficients due to its small effective area is more challenging [30]. Besides, in the field of telecommunication and supercontinuum applications nonlinearity with high birefringence derived a massive interest [31].

In this paper, a microstructure core based photonic crystal fiber is proposed that shows high birefringence, high relative sensitivity and lower confinement loss at the same time. The proposed PCF contains five rings of air holes in the cladding where the core contains elliptical air holes. The air holes of cladding are kept same to avoid design complexities. The proposed PCF shows 53.07% relative sensitivity as a gas sensor. Besides, the PCF shows high birefringence of 6.9×10^{-3} and lower confinement loss of 3.21×10^{-6} , the high nonlinearity of $15.67 \text{ W}^{-1}\text{km}^{-1}$ at the wavelength of $1.33 \mu\text{m}$. V parameters show the proposed PCF is a single mode fiber with a large effective area $3.88 \mu\text{m}^2$ at the wavelength $1.33 \mu\text{m}$. In addition, splice loss and beat length are also analyzed. A large number of analyses of the guiding and optical properties of PCF take place in this paper which makes our research unique one.

2. Geometries of the proposed E-PCF

Fig. 1 shows the transverse cross-sectional view of the proposed E-PCF. The cladding contains five rings of air holes in hexagonal manner. This method was introduced by [25] where the cladding was hexagonal with six missing holes in the edges of the outermost cladding. The diameters of two outermost ring and the three innermost rings were not same in the work. In our proposed E-PCF the diameters of all the five rings of cladding were kept same to match the proper fabrication tolerance and assumed as d . The concept of microstructure core was introduced by [24]. In [26] elliptical holes were used to get high birefringence. In the proposed E-PCF the core is organized with an array of 8 elliptical air holes which is horizontally arranged. The major and minor axis of the elliptical air holes is defined as d_a and d_b respectively. The hole to hole distance of two adjacent air holes is called pitch. The pitch between the holes of core and the holes of cladding is defined as Λ_1 and Λ respectively. By article [25], the diameters of the innermost ring are responsible for high sensitivity and the diameters of outermost rings are responsible for lower confinement loss. In our proposed E-PCF the cladding air holes are optimized bigger to attain the low confinement loss and make the proper interaction of light through the core. All the parameters of both core and cladding were optimized by varying as a function of wavelength. By using perfectly matched layer (PML) boundary condition the optical properties and propagation

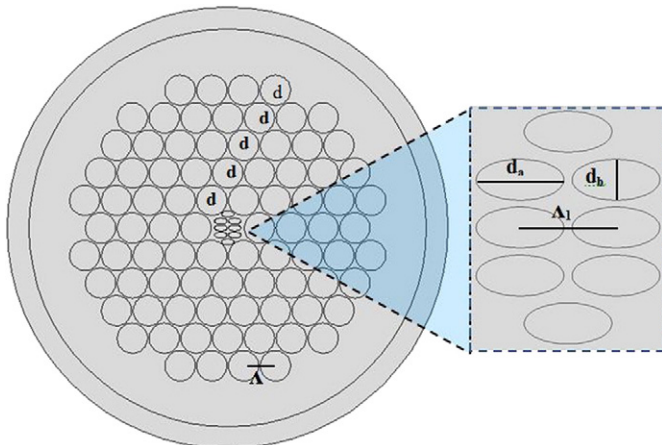


Fig. 1. Transverse cross section of the proposed E-PCF.

characteristics of leaky mode can be measured. The PML is set 10% of the total diameter of the proposed E-PCF to meet the boundary condition.

3. Synopsis of the simulation method

A finite element method (FEM) is used for solving Maxwell's Equation to simulate the guiding properties of the proposed PCF. It can solve very complex structures and can provide full vector analysis of different PCF structure [32].

To calculate the evanescent field by the gas samples the Beer-Lambert law can be used. The relationship between optical intensity and gas concentration can be determined as:

$$I(\lambda) = I_0(\lambda) \exp[-r\alpha_m l_c] \quad (1)$$

The absorbance of the sample can be defined as:

$$A = \log\left(\frac{I}{I_0}\right) = r\alpha_m l_c \quad (2)$$

Here, α_m is the absorption coefficient of the gas being detected; l is the length of the PCF; c is the gas concentration. Output light intensities with and without the presence of gas are I and I_0 respectively. Relative sensitivity r can be defined as:

$$r = \frac{n_s}{\text{Re}[n_{\text{eff}}]} f \quad (3)$$

where n_s is the refractive index of gas species considered 1; $\text{Re}[n_{\text{eff}}]$ is the real part of the effective mode index. Here f is the fraction of total power and hole power which can be defined as:

$$f = \frac{\int_{\text{holes}} \text{Re}(E_x H_y - E_y H_x) dx dy}{\int_{\text{total}} \text{Re}(E_x H_y - E_y H_x) dx dy} \quad (4)$$

Here, E_x , E_y , H_x and H_y are the transverse electric and magnetic field. A circular perfectly matched layer (PML) is used to fulfill the boundary condition which avoids possible reflection at the boundary. By this term confinement loss or leakage loss can be calculated by the imaginary part of the effective refractive index. The confinement loss or leakage loss can be calculated by the following equation:

$$L_c = 8.868 \times K_0 I_m[n_{\text{eff}}] (\text{dB/m}) \quad (5)$$

where, K_0 is the wavenumber and $I_m[n_{\text{eff}}]$ is the imaginary part of the effective refractive index. The difference between refractive index of x-polarization and y-polarization is called the birefringence which can be defined as:

$$B = |n_x - n_y| \quad (6)$$

This property leads to periodic power exchange between two orthogonal components. This period is beat length which can be determined by:

$$L_B(\lambda) = \lambda/B(\lambda) \quad (7)$$

The single mode response can be determined by the V-parameter which is defined by:

$$V_{\text{eff}} = \frac{2\pi r f}{c} \sqrt{n_{\text{co}}^2 - n_{\text{cl}}^2} \leq 2.405 \quad (8)$$

Here, n_{co} and n_{cl} are the refractive indexes of core and cladding. V-parameter (V_{eff}) of a PCF must be less than or equal 2.405 to be a

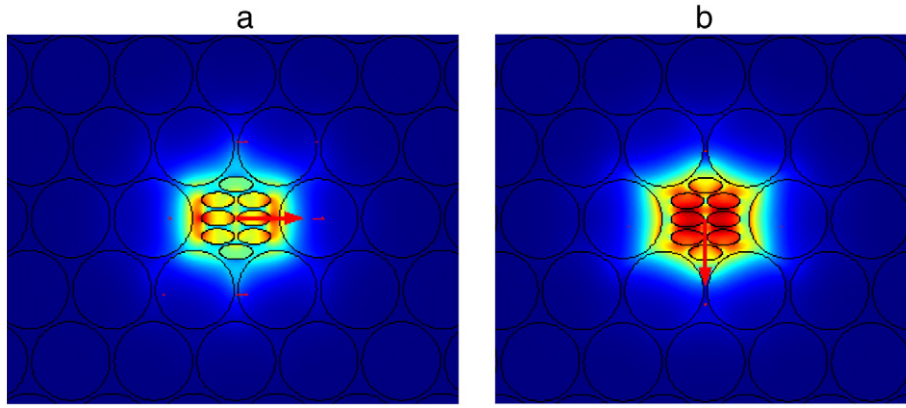


Fig. 2. Mode field pattern of proposed PCF for (a) x-polarization (b) y-polarization at $\lambda = 1.33 \mu\text{m}$.

single mode fiber. The effective area [33] of a PCF can be determined by the following equation:

$$A_{\text{eff}} = \frac{(\iint |E|^2 dx dy)^2}{\iint |E|^4 dx dy} \quad (9)$$

High optical power density is provided by a small effective area for which the nonlinear effect to be significant. The nonlinear coefficient [34] can be examined by the following:

$$\gamma = \left(\frac{2\pi}{\lambda}\right) \left(\frac{n_2}{A_{\text{eff}}}\right) \quad (10)$$

Here, n_2 is the nonlinear refractive index. Splice loss occurs during the splicing of the photonic crystal fiber and the single mode fiber. Splice loss can be calculated by the following equation:

$$L_s = -20 \log_{10} \frac{2W_{\text{SMF}}W_{\text{EPCF}}}{W_{\text{SMF}}^2 + W_{\text{EPCF}}^2} \quad (11)$$

Here, W_{SMF} and $W_{\text{E-PCF}}$ are the mode field diameters of the single mode fiber and the proposed E-PCF respectively. The background material was set pure silica whose refractive index changes with the variation of the wavelength according to the Sellmeier equation.

$$n(\lambda) = \sqrt{\left(1 + \frac{B_1\lambda^2}{\lambda^2 - C_1} + \frac{B_2\lambda^2}{\lambda^2 - C_2} + \frac{B_3\lambda^2}{\lambda^2 - C_3}\right)} \quad (12)$$

Here, $n(\lambda)$ is the refractive index of silica which varies with the operating wavelength and $B_{(i=1,2,3)}$ and $C_{(i=1,2,3)}$ are Sellmeier coefficients.

4. Results and discussion

The mode field pattern along the x-polarization and y-polarization of the proposed E-PCF has been shown in Fig. 2. From the figure, it can be demonstrated that the mode field is tightly confined to the core region. So the leakage loss will be very low.

Fig. 3 depicts the comparisons of sensitivity and confinement loss of the proposed PCF with prior PCF1 [24], PCF2 [23] and PCF3 [35] respectively. The proposed PCF for optimized parameters shows higher sensitivity and lower confinement loss comparing to prior PCFs. Optimizing the parameters, sensitivity and confinement loss coefficients of 53.07% and 3.21×10^{-6} dB/m are obtained at 1.33 μm wavelength for x-polarized mode respectively. To optimize the different parameters a simple technique has been followed on the proposed E-PCF. To calculate the confinement loss efficiently, proposed structure thickness is fixed at 10% of the fiber radius by PML test. But no significant effect on relative sensitivity has been noticed for the proposed thickness about 1.5 μm . By selecting a fine mode of mesh size, the simulation work has been completed using 4.2 version COMSOL Multiphysics. Convergence error, defective modes in PCF with compactly supported perturbations, is very low about $2.71 \times 10^{-6}\%$. First, air filling ratio (d/Λ) is varied to 0.447, 0.460 and 0.475 μm keeping other parameters constant.

From Fig. 4 it is clearly depicted that sensitivity increases as the air filling ratio increases, for example, at 1.33 μm wavelength, the sensitivity is 43.71%, 48.23%, 53.07%; the confinement loss is 1.35×10^{-5} dB/m,

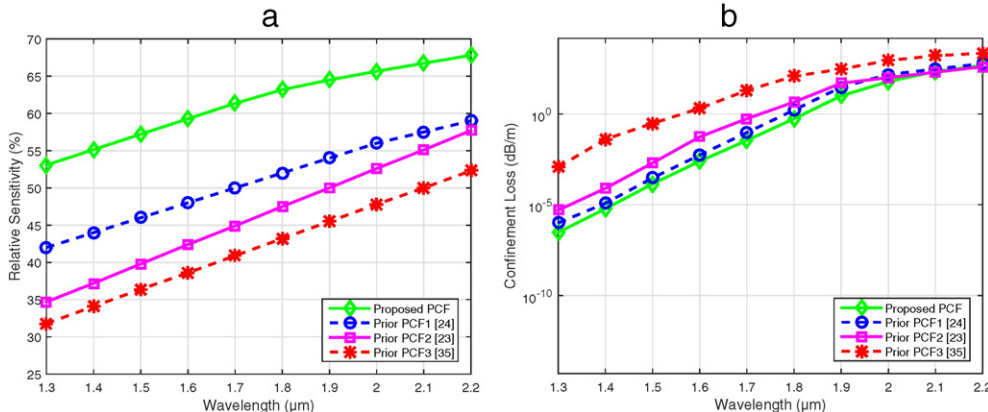


Fig. 3. Comparison of (a) relative sensitivity (b) confinement loss for the optimized parameters of the proposed PCF with the prior PCFs.

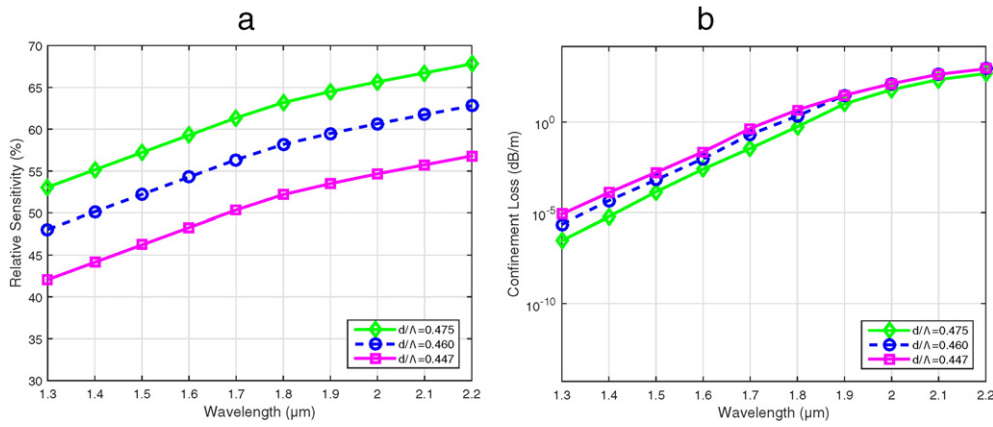


Fig. 4. Variation of (a) relative sensitivity (b) confinement loss as a function of wavelength for $d/\Lambda = 0.475$, $d/\Lambda = 0.460$ and $d/\Lambda = 0.447$ while other parameters are kept constant.

7.37×10^{-5} dB/m, 3.21×10^{-6} dB/m and the birefringence is 1.23×10^{-3} , 5.31×10^{-3} , 6.9×10^{-3} for $d/\Lambda = 0.475$, 0.460 and $0.447 \mu\text{m}$ respectively. So it is also clearly visualized that the proposed PCF shows higher sensitivity as well as higher birefringence for $d/\Lambda = 0.475 \mu\text{m}$ shown in Fig. 6 (a). Simultaneously the higher birefringence and sensitivity makes a fiber as a potential candidate to detect colorless and noxious gasses as well as environment pollution monitoring [13]. Now $d/\Lambda = 0.475 \mu\text{m}$ is selected for further investigation process.

Fig. 5 demonstrates the sensitivity and confinement loss dependency on the pitch of the cladding of proposed E-PCF. According to Fig. 5 and

Fig. 6 (b), Λ (pitch) variation has the major impact on sensitivity, confinement loss as well as birefringence. Pitch, $\Lambda = 1.70$, 1.65 and $1.60 \mu\text{m}$ is selected for investigation. The sensitivity is 39.78%, 46.62% and 53.07%; the confinement loss is 1.01×10^{-5} dB/m, 6.17×10^{-5} dB/m, and 3.21×10^{-6} dB/m and the birefringence is 0.51×10^{-1} , 6.71×10^{-2} and 6.9×10^{-3} for selected pitches respectively at $\lambda = 1.33 \mu\text{m}$. Finally, it is clearly noticed that $\Lambda = 1.60 \mu\text{m}$ obtains better-guiding properties and selected for next investigation.

Fig. 7 exhibits the variation of d_a/d_b on investigated guiding properties. The $d_a/d_b = 0.464$, 0.467 and 0.469 are used to investigate the

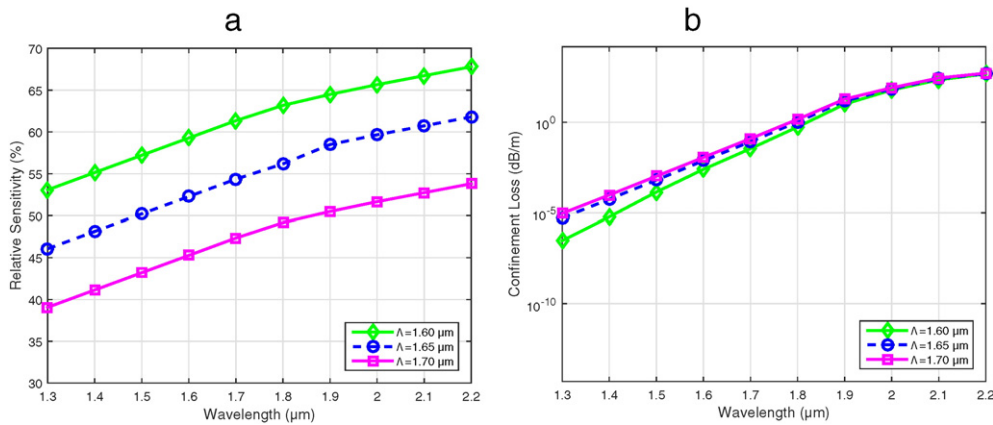


Fig. 5. Variation of (a) relative sensitivity (b) confinement loss as a function of wavelength for $\Lambda = 1.60 \mu\text{m}$, $\Lambda = 1.65 \mu\text{m}$ and $\Lambda = 1.70 \mu\text{m}$ while other parameters are kept constant.

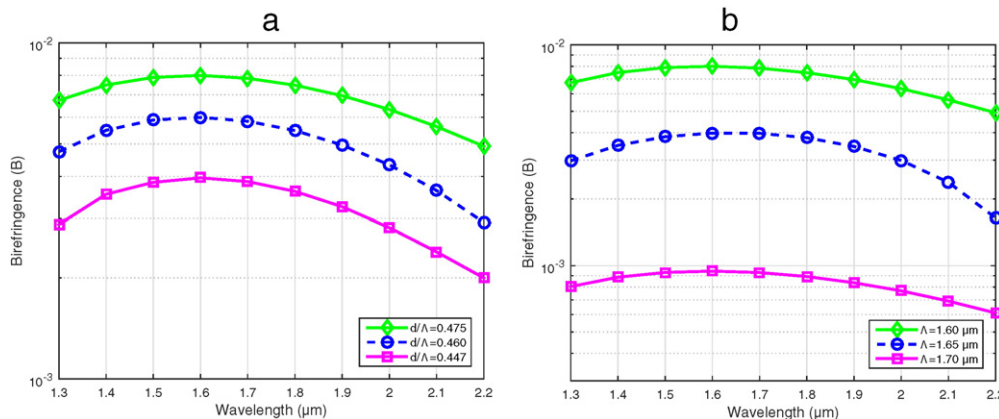


Fig. 6. Variation of birefringence as a function of wavelength for $\Lambda = 1.60 \mu\text{m}$, $\Lambda = 1.65 \mu\text{m}$ and $\Lambda = 1.70 \mu\text{m}$ while other parameters are kept constant.

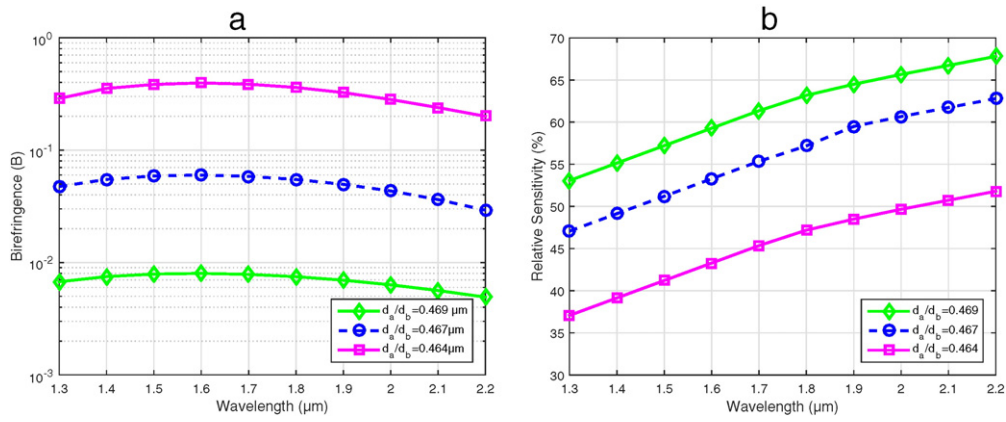


Fig. 7. Variation of (a) relative sensitivity (b) birefringence as a function of wavelength for $d_a/d_b = 0.469$, $d_a/d_b = 0.467$, $d_a/d_b = 0.464$ while other parameters are kept constant.

guiding properties. From the Fig. 7 it is clearly reported that better guiding properties are gained for $d_a/d_b = 0.469$. The sensitivity, confinement loss, and birefringence are obtained 53.07%, 3.21×10^{-6} dB/m and 6.9×10^{-3} respectively for $d_a/d_b = 0.469$. After competition of simulation process investigating the effects of different parameters on proposed PCF, it is nicely addressed that the relative sensitivity can be enhanced due to the global diameter increment is shown in Table 1. Better sensitivity proves more confine of light in the core area and also the better electromagnetic power interaction with gasses. Investigated results highlight that interaction between light and gasses increases through wavelength increases. Finally, the air filling ratio $d/\Lambda = 0.475$ μm, pitch $\Lambda = 1.60$ μm and $d_a/d_b = 0.469$ are chosen as optimum values. For these optimum values, we have observed the other optical properties of the proposed E-PCF.

Table 1
Comparison of different index-guiding properties for optimum design parameters and also for fiber's global diameter variations of order $\pm 1-2\%$ around the optimum value.

| Change in diameters (%) | Relative sensitivity (%) | Confinement loss (dB/m) | Birefringence (B) |
|-------------------------|--------------------------|-------------------------|----------------------|
| +2 | 57.31 | 2.32×10^{-7} | 6.4×10^{-3} |
| +1 | 55.03 | 7.41×10^{-7} | 6.7×10^{-3} |
| Optimum | 53.07 | 3.21×10^{-6} | 6.9×10^{-3} |
| -1 | 52.94 | 3.71×10^{-5} | 6.8×10^{-3} |
| -2 | 50.08 | 5.75×10^{-5} | 6.5×10^{-3} |

The relative sensitivity curve of the different core formation of our proposed E-PCF was analyzed in Fig. 8. To investigate the core region we fixed the cladding and took different core formation to ensure the effectiveness. We have selected circular holes in a circular form and set it as core to investigate. Besides, elliptical holes in an array and the formation of proposed E-PCF is also analyzed. From all the investigated results it can illustrate that the arrangements of elliptical holes in the proposed E-PCF show higher sensitivity than the other organizations of holes in the core region.

According to Eqs. 9 and 10, Fig. 9 represents the wavelength dependence of effective areas and nonlinear coefficient of the fiber respectively for the optimized parameters. The nonlinear coefficient and effective areas of the proposed fiber are $15.67 \text{ W}^{-1}\text{km}^{-1}$ and 3.88 μm^2 respectively at 1.33 μm wavelength. The nonlinear coefficient of the fiber is high but relatively poor compare with [36] alike effective areas. The small effective area associates potential difficulties in the I/O coupling of light as well as higher splicing loss. 0.1 dB taper losses have been reported to interface PCFs and conventional SMFs using a tapered intermediate PCF mode matched both of fiber at every end [37]. Due to the geometrical shape of the proposed PCF shown in Fig. 1, the fiber supports only single mode. Through the operating wavelengths (1.3–2.2 μm) V_{eff} remains always below 2.405 of the optimized PCF shown in Fig. 10. Construction manner is another possible solution to reduce the splice loss with PCFs to conventional SMFs [13]. The splice loss of proposed PCF is 8.21 dB at 1.33 μm wavelength shown in Fig. 11 for optimum design parameters.

A beat length of about 0.198 mm is confirmed at the wavelength of 1.33 μm. A splice-free interconnection technique has been proposed by Lean-Saval et al. [38] between PCFs and conventional SMFs which

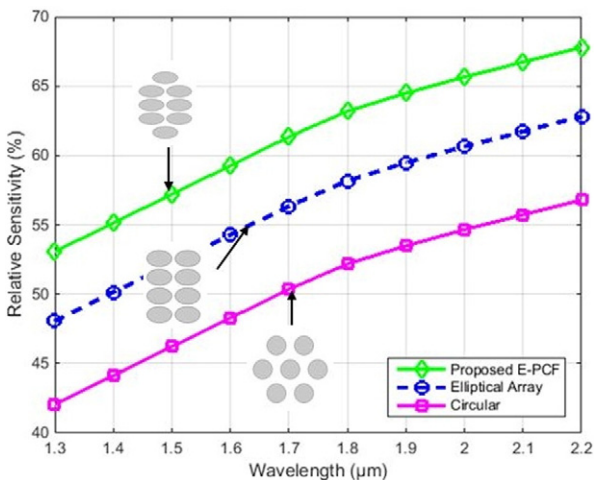


Fig. 8. Variation of relative sensitivity as a function of wavelength among different core formation of the proposed PCF.

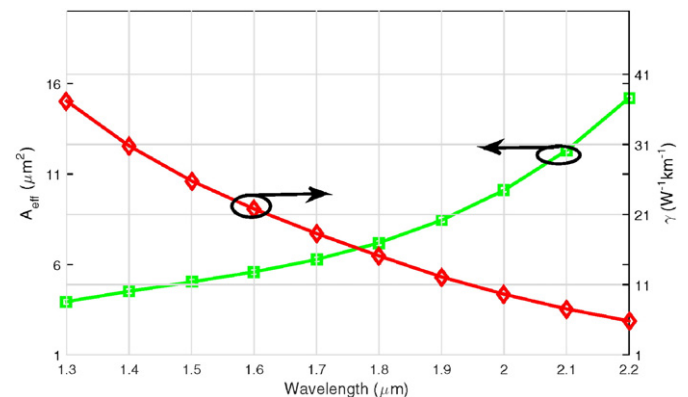


Fig. 9. Wavelength dependence of effective area and nonlinear coefficient for the optimized parameters of proposed PCF.

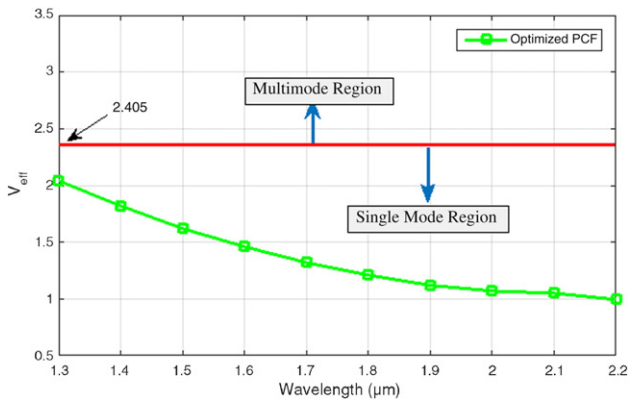


Fig. 10. Wavelength dependence of V parameter values for single mode test for the optimized parameters of proposed E-PCF.

can be used to interface the proposed PCFs with existing technology without a major problem.

Table 1 shows the investigated guiding properties of the proposed fiber for the optimum design parameters and for the global diameters variations of the order of $\pm 1\%$ to $\pm 2\%$ at $1.33 \mu\text{m}$ wavelength. From Table 1, it is nicely visualized for the optimizing geometrical parameters of the proposed PCF that a high relative sensitivity of 53.07%, the birefringence of 6.9×10^{-3} is confirmed both at $\lambda = 1.33 \mu\text{m}$. The investigated birefringence is much higher than conventional PM fibers [39]. Now the higher birefringence fiber can be applied to reduce the effect of polarization mode in sensing applications. Supporting the linear polarization will be another skill of our proposed PCF which minimizes the polarization coupling problem [13].

During the fabrication process, 1% variations of global diameters in the fiber may occur where 2% is tolerable [37]. It is clearly reported in Table 1 that there are no much changes of investigated guiding properties value for $\pm 1\%$ variations of global parameters. So after fabrication process, there will be little bit performance variations of proposed PCF.

In a particular wavelength, each gas has its own absorption line. To detect gasses in remote places low loss optical fibers in the near infrared region (NIR) can be used which have minimum transmission loss ($<1 \text{ dB/km}$) [23]. The absorption line of methane (CH_4) and hydrogen fluoride (HF) is the wavelength of $1.33 \mu\text{m}$. In this paper, we mainly focused on these to gasses methane (CH_4) and hydrogen fluoride (HF). Besides, the proposed PCF can detect the gasses of a different absorption line of a wide range of wavelength from $1.33 \mu\text{m}$ to $2.2 \mu\text{m}$.

For sensing application and fiber loop mirror high birefringent PCFs (HB-PCFs) are suitable. Elliptical holes provide high birefringence of PCF which has better polarization maintenance properties. Few applications like stabilizing the operation of optical devices and extinguishing the consequences of polarization mode dispersion PCFs with PM properties is needed [40]. The proposed E-PCF shows higher birefringence than the conventional PM fibers. Besides, the proposed PCF shows lower confinement loss or leakage loss. In order to decrease confinement loss, the number of rings of air holes in cladding must be increased. Additionally, confinement loss may be zero if there are infinite numbers of holes in the cladding but this scheme is not practically adjustable.

Fabrication is an important and challenging issue of any photonic crystal fiber. Our proposed PCF is a dual shape mixing PCF (core holes are elliptical and cladding holes are circular). Authors believe that due to the advancement of the fabrication process of nanotechnology the proposed E-PCF can be fabricated in recent years. To gain ultrahigh birefringence such types of dual shape mixing PCF was proposed [41] in the past. To fabricate our proposed E-PCF different types of fabrication process can be used (one to fabricate core region and another to fabricate cladding region). Elliptical holes can be successfully fabricated in recent years [42]. Besides, a capillary stacking method [43] can be used to fabricate the proposed E-PCF. The sol-gel method can be used especially for

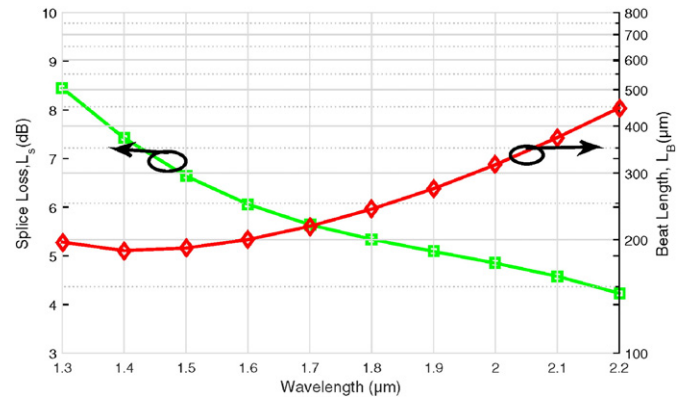


Fig. 11. Wavelength dependence of splice loss and beat length for the optimized parameters of proposed E-PCF.

fabrication of the cladding because this method allows PCF to fabricate with different holes shapes and size [44].

5. Conclusion

We have proposed a micro-cored based photonic crystal fiber gas sensor with high sensitivity, birefringence low confinement loss consequently between the wider wavelength ranges from $1.3 \mu\text{m}$ to $2.2 \mu\text{m}$. In proposed E-PCF, the core is formulated with elliptical holes. The variation of index guiding properties on the proposed fiber parameters is numerically investigated applying FEM and perfectly matched layer (PML) circular boundary condition. The proposed fiber exhibits sensitivity, birefringence, nonlinear coefficient, effective area as high as 53.07%, 6.9×10^{-3} , $15.67 \text{ W}^{-1}\text{km}^{-1}$, $3.88 \mu\text{m}^2$ respectively. The higher sensitivity makes this fiber a potential candidate to detect colorless and toxic gasses as well as environment pollution monitoring. In addition, the proposed E-PCF will be helpful in other sensing applications and overcome the critical trade-off among investigated index-guiding properties. Moreover, fiber loop mirror, polarization control, four wave mixing, telecommunication application and fiber optic sensor can be the efficient uses of the accounted results.

Acknowledgment

The authors are grateful to those who participated in research.

References

- [1] J.C. Knight, Photonic crystal fibers, *Nature* 424 (6950) (2003) 847–851.
- [2] J.C. Knight, J. Broeng, T.A. Birks, P.S.J. Russell, Photonic band gap guidance in optical fiber, *Science* 282 (1998) 1476–1478.
- [3] J.M. Fini, Microstructure fibers for optical sensing in gasses and liquids, *Meas. Sci. Technol.* 15 (2004) 1120–1128.
- [4] J.C. Knight, T.A. Birks, P.S.J. Russell, D.M. Atkin, All-silica single-mode optical fiber with photonic crystal cladding, *Opt. Lett.* 21 (1996) 1547–1549.
- [5] T.A. Birks, J.C. Knight, P.S.J. Russell, Endlessly single-mode photonic crystal fiber, *Opt. Lett.* 22 (1997) 961–963.
- [6] J.C. Knight, T.A. Birks, P.S.J. Russell, D.M. Atkin, All-silica single-mode optical fiber with photonic crystal cladding, *Opt. Lett.* 21 (19) (1996) 1547–1549.
- [7] H. Ademgil, Highly sensitive octagonal photonic crystal fiber based sensor, *Optik-International Journal for Light and Electron Optics* 125 (2014) 6274–6278.
- [8] S.A. Razzak, M.A.G. Khan, F. Begum, S. Kaijage, Guiding properties of a decagonal photonic crystal fiber, *Journal of Microwaves, Optoelectronics, and Electromagnetic Applications (JMOE)* 6 (1) (2007) 44–49.
- [9] Y. Hou, F. Fan, Z.-W. Jiang, X.-H. Wang, S.-J. Chang, Highly birefringent polymer terahertz fiber with honeycomb cladding, *Optik-International Journal for Light and Electron Optics* 124 (17) (2013) 3095–3098.
- [10] S. Asaduzzaman, M.F.H. Arif, K. Ahmed, P. Dhar, Highly sensitive simple structure circular photonic crystal fiber-based chemical sensor, 2015 IEEE International WIE Conference on Electrical and Computer Engineering (WIECON-ECE) 2015, pp. 151–154.
- [11] M. Morshed, M.F.H. Arif, S. Asaduzzaman, K. Ahmed, Design and characterization of photonic crystal fiber for sensing applications, *European Scientific Journal* 11 (12) (2015).

- [12] M. Morshed, M.I. Hasan, S.A. Razzak, Enhancement of the sensitivity of gas sensor based on microstructured optical fiber, *Photonic Sensors* 5 (2015) 312–320.
- [13] M.S. Habib, M.S. Habib, S.A. Razzak, M.A. Hossain, Proposal for highly birefringent broadband dispersion compensating octagonal photonic crystal fiber, *Opt. Fiber Technol.* 19 (2013) 461–467.
- [14] M.S. Habib, M.S. Habib, M.I. Hasan, S.A. Razzak, A single mode ultra flat high negative residual dispersion compensating photonic crystal fiber, *Opt. Fiber Technol.* 20 (2014) 328–332.
- [15] F. Begum, Y. Namihira, S.A. Razzak, S. Kaijage, N.H. Hai, T. Kinjo, K. Miyagi, N. Zou, Design and analysis of novel highly nonlinear photonic crystal fibers with ultra-flattened chromatic dispersion, *Opt. Commun.* 282 (2009) 1416–1421.
- [16] F. Zolla, G. Renversez, A. Nicolet, B. Kuhlmeiy, S. Guenneau, D. Felbacq, A. Argyros, S. Leon-Saval, *Foundations of photonic crystal fibers*, World Scientific, 2005.
- [17] H. Ebendorff-Heidepriem, P. Petropoulos, S. Asimakis, V. Finazzi, R. Moore, K. Frampton, F. Koizumi, D. Richardson, T. Monro, Bismuth glass holey fibers with high nonlinearity, *Opt. Express* 12 (21) (2004) 5082–5087.
- [18] C. Lecaplain, B. Ortaç, G. Machinet, J. Boulet, M. Baumgartl, T. Schreiber, E. Cormier, A. Hideur, High-energy femtosecond photonic crystal fiber laser, *Opt. Lett.* 35 (19) (2010) 3156–3158.
- [19] R. Holzwarth, T. Udem, T.W. Hänsch, J.C. Knight, W.J. Wadsworth, P.S.J. Russell, Optical frequency synthesizer for precision spectroscopy, *Phys. Rev. Lett.* 85 (11) (2000) 2264.
- [20] J.M. Dudley, G. Genty, S. Coen, Supercontinuum generation in photonic crystal fiber, *Rev. Mod. Phys.* 78 (4) (2006) 1135.
- [21] M. Morshed, S. Asaduzzaman, M.F.H. Arif, K. Ahmed, Proposal of simple gas sensor based on micro structure optical fiber, *Electrical Engineering and Information Communication Technology (ICEEICT)*, 2015 International Conference on 2015, pp. 1–5.
- [22] C. Cordeiro, M.A. Franco, G. Chesini, E. Barretto, R. Lwin, C.H. Brito Cruz, M.C. Large, Microstructured-core optical fiber for evanescent sensing applications, *Opt. Express* 14 (2006) 13056–13066.
- [23] S. Olyae, A. Naraghi, Design and optimization of the index-guiding photonic crystal fiber gas sensor, *Photonic Sensors* 3 (2) (2013) 131–136.
- [24] M. Morshed, M.I. Hassan, T.K. Roy, M.S. Uddin, S.A. Razzak, Microstructure core photonic crystal fiber for gas sensing applications, *Appl. Opt.* 54 (2015) 8637–8643.
- [25] S. Olyae, A. Naraghi, V. Ahmadi, High sensitivity evanescent field gas sensor based on modified photonic crystal fiber for gas condensate and air pollution monitoring, *Optik-International Journal for Light and Electron Optics* 125 (2014) 596–600.
- [26] H. Ademgil, S. Haxha, PCF based sensor with high sensitivity, high birefringence and low confinement losses for liquid analyte sensing applications, *Sensors* 15 (2015) 31833–31842.
- [27] M.I. Hasan, M.S. Habib, M.S. Habib, S.A. Razzak, Highly nonlinear and highly birefringent dispersion compensating photonic crystal fiber, *Opt. Fiber Technol.* 20 (1) (2014) 32–38.
- [28] D. Chen, L. Shen, Ultrahigh birefringent photonic crystal fiber with ultralow confinement loss, *IEEE Photon. Technol. Lett.* 19 (2007) 185–187.
- [29] Y. Yue, G. Kai, Z. Wang, T. Sun, L. Jin, Y. Lu, C. Zhang, J. Liu, Y. Li, Y. Liu, et al., Highly birefringent elliptical-hole photonic crystal fiber with squeezed hexagonal lattice, *Opt. Lett.* 32 (5) (2007) 469–471.
- [30] H. Ademgil, S. Haxha, F. Abdel Malek, et al., Highly nonlinear bending-insensitive birefringent photonic crystal fibres, *Engineering* 2 (8) (2010) 608.
- [31] S.A. Razzak, Y. Namihira, Proposal for highly nonlinear dispersion-flattened octagonal photonic crystal fibers, *IEEE Photon. Technol. Lett.* 20 (4) (2008) 249–251.
- [32] T.M. Monro, W. Belardi, K. Furusawa, J.C. Baggett, N.G.R. Broderick, D.J. Richardson, Sensing with microstructured optical fibers, *Meas. Sci. Technol.* 12 (7) (2001) 854.
- [33] M.S. Habib, M.S. Habib, S.A. Razzak, Y. Namihira, M.A. Hossain, M.G. Khan, Broadband dispersion compensation of conventional single-mode fibers using microstructure optical fibers, *Optik-International Journal for Light and Electron Optics* 124 (19) (2013) 3851–3855.
- [34] S. Coen, A.H.L. Chau, R. Leonhardt, J.D. Harvey, J.C. Knight, W.J. Wadsworth, P.S.J. Russell, White-light supercontinuum generation with 60-ps pump pulses in a photonic crystal fiber, *Opt. Lett.* 26 (17) (2001) 1356–1358.
- [35] Z. Zhi-guo, Z. Fang-di, Z. Min, Y. Pei-da, Gas sensing properties of index-guided PCF with air-core, *Opt. Laser Technol.* 40 (1) (2008) 167–174.
- [36] M.S. Habib, M.S. Habib, M.I. Hasan, S.M.A. Razzak, Tailoring polarization maintaining broadband residual dispersion compensating octagonal photonic crystal fibers, *Opt. Eng.* 52 (11) (2013) 116111.
- [37] T.A. Birks, G. Kakarantzas, P.S.J. Russell, Presented at *Opt. Fiber Commun. Con. Paper ThK2*, 2004.
- [38] S.G. Leon-Saval, T.A. Birks, N.Y. Joy, A.K. George, W.J. Wadsworth, G. Kakarantzas, P.S.J. Russell, Splice-free interfacing of photonic crystal fibers, *Opt. Lett.* 30 (2005) 1629–1631.
- [39] G. Agrawal, *Nonlinear Fiber Optics*, 2nd ed. Academic press, San Diego, California.
- [40] P. Francesco, V. Finazzi, T.M. Monro, N.G. Broderick, V. Tse, D.J. Richardson, Inverse design and fabrication tolerances of ultra-flattened dispersion holey fibers, *Opt. Express* 13 (10) (2005) 3728–3736.
- [41] M.S. Habib, M.S. Habib, S.A. Razzak, M.A. Hossain, Proposal for highly birefringent broadband dispersion compensating octagonal photonic crystal fiber, *Opt. Fiber Technol.* 19 (5) (2013) 461–467.
- [42] N.A. Issa, M.A. Eijkelenborg, C.F. FellowM, G. Henry, M.C. Large, Fabrication and study of microstructured optical fibers with elliptical holes, *Opt. Lett.* 29 (2004) 1336–1338.
- [43] A. Argyros, I. Bassett, M. Eijkelenborg, M. Large, J. Zagari, N.A. Nicorovici, R. McPhedran, C.M. Sterke, Ring structures in microstructured polymer optical fibers, *Opt. Express* 9 (2001) 813–820.
- [44] R.T. Bise, D.J. Trevor, Sol-gel derived microstructured fiber: fabrication and characterization, Presented in *Optical Fiber Communications Conf. (OFC)*, 2005.